Journal of Molecular and Cellular Cardiology 155 (2021) 1–9

Contents lists available at ScienceDirect

Journal of Molecular and Cellular Cardiology

journal homepage: www.elsevier.com/locate/yjmcc

Original article

Global identification of S-palmitoylated proteins and detection of palmitoylating (DHHC) enzymes in heart

Madeleine R. Miles [a], John Seo [a], Min Jiang [a], Zachary T. Wilson [a], Janay Little [a,1], Jon Hao [b], Joshua Andrade [c], Beatrix Ueberheide [c,d,e], Gea-Ny Tseng [a,*]

[a] Department of Physiology & Biophysics, Virginia Commonwealth University, Richmond, VA, United States
[b] Poochon Scientific, Frederick, MD, United States
[c] Proteomics Laboratory, Division of Advance Research Technology, New York University, School School of Medicine, New York, NY, United States
[d] Department of Biochemistry and Molecular Pharmacology, New York University, School of Medicine, New York, NY, United States
[e] Department of Neurology, New York University, School of Medicine, New York, NY, United States

ARTICLE INFO

Keywords:
Palmitoylation
Protein palmitoyl transferase
Proteomics
Cardiac disease

ABSTRACT

High-throughput experiments suggest that almost 20% of human proteins may be S-palmitoylatable, a post-translational modification (PTM) whereby fatty acyl chains, most commonly palmitoyl chain, are linked to cysteine thiol groups that impact on protein trafficking, distribution and function. In human, protein S-palmitoylation is mediated by a group of 23 palmitoylating 'Asp-His-His-Cys' domain-containing (DHHC) enzymes. There is no information on the scope of protein S-palmitoylation, or the pattern of DHHC enzyme expression, in the heart. We used resin-assisted capture to pull down S-palmitoylated proteins from human, dog, and rat hearts, followed by proteomic search to identify proteins in the pulldowns. We identified 454 proteins present in at least 2 species-specific pulldowns. These proteins are operationally called 'cardiac palmitoylome'. Enrichment analysis based on Gene Ontology terms 'cellular component' indicated that cardiac palmitoylome is involved in cell-cell and cell-substrate junctions, plasma membrane microdomain organization, vesicular trafficking, and mitochondrial enzyme organization. Importantly, cardiac palmitoylome is uniquely enriched in proteins participating in the organization and function of t-tubules, costameres and intercalated discs, three microdomains critical for excitation-contraction coupling and intercellular communication of cardiomyocytes. We validated antibodies targeting DHHC enzymes, and detected eleven of them expressed in hearts across species. In conclusion, we provide resources useful for investigators interested in studying protein S-palmitoylation and its regulation by DHHC enzymes in the heart. We also discuss challenges in these efforts, and suggest methods and tools that should be developed to overcome these challenges.

1. Introduction

Protein S-palmitoylation (also known as S-acylation) is a form of post-translational modification, whereby a long fatty acyl chain, usually palmitoyl chain, is attached to thiol side chain of cysteine (Cys) residues in proteins [1]. The resulting increase in local hydrophobicity promotes binding of cytosolic proteins to organelle or plasma membranes [2,3]. S-palmitoylation of integral membrane proteins can promote their segregation into liquid-ordered (raft) domains [2,3]. Therefore, S-palmitoylation impacts on proteins' distribution and function.

Due to the advancement in experimental techniques for detecting and quantifying protein S-palmitoylation [4–6], our understanding of the scope and functional roles of protein S-palmitoylation has progressed profoundly in recent years. High-throughput experiments have defined palmitoyl-proteomes (abbreviated as 'palmitoylomes' herein) of various cell types and from different species [7]. The current version of SwissPalm, a public repository of information on protein palmitoylation reports 4587 human proteins collectively identified in 17 human palmitoylomes, accounting for 19.5% of 23,484 human proteins in its database. The prevalence of protein S-palmitoylation indicates that this PTM is involved in many aspects of cellular function.

Protein S-palmitoylation is mediated by the so-called DHHC (or

* Corresponding author at: Department of Physiology & Biophysics, Virginia Commonwealth University, Richmond, VA 23298, United States.
E-mail address: gea-ny.tseng@vcuhealth.org (G.-N. Tseng).
[1] Current affiliation: Department of Biochemistry & Molecular Biology, Virginia Commonwealth University, Richmond, VA, United States

https://doi.org/10.1016/j.yjmcc.2021.02.007
Received 7 November 2020; Received in revised form 12 February 2021; Accepted 15 February 2021
Available online 23 February 2021

zDHHC) enzymes, because of their shared aspartate-histidine-histidine-cysteine, or 'DHHC', motif [1]. Human has 23 DHHC genes [1]. Mutations in DHHC genes have been linked to neurological disorders and cancers [1], pointing to their importance in human physiology and diseases. Efforts have been under way to design small molecule DHHC modulators as therapeutic agents for human disorders [8].

There is no information on the scope of protein S-palmitoylation, or the pattern of DHHC enzyme expression, in the heart. Such information is important for a better understanding of human heart physiology and pathophysiology, and the ability to design novel therapeutic interventions for cardiac disorders. For example, it has been suggested that S-palmitoylation is involved in a process called 'massive endocytosis' or MEND, that occurs to cardiomyocytes experiencing ischemia/reperfusion (I/R) injury [9]. MEND negatively impacts cardiomyocyte recovery after I/R injury. Knocking down a palmitoylating enzyme, DHHC5, expressed in the heart appears to protect cardiomyocytes against MEND [9]. Another example is DHHC2, shown to be one of 35 consistently upregulated genes, dubbed 'gene expression signatures', in coronary heart disease [10]. These observations suggest that inhibiting DHHC5 or DHHC2 may offer therapeutic benefits against cardiac injury. But, what are their substrates in the heart? What may be the side effects of inhibiting them?

The goal of this 'resource' article is to provide useful information for investigators interested in studying protein S-palmitoylation and its regulation by DHHC enzymes in the heart. To reach this goal, we first investigated the scope of protein S-palmitoylation in the heart. Currently, only a small number of cardiac proteins are known to be S-palmitoylated: Nav1.5 [11], Kv1.5 [12], K channel interacting protein 2 'KChIP2' [13], Kir6.2 [14], Cavβ2a [15], Na/Ca exchanger 1 'NCX1' [16], phospholamban 'PLN' [17], endothelial nitric oxide synthase 'eNOS' [18], phospholemman 'PLM' [19], caveolin-3 'Cav-3' [20], desmosomal components (desmoglein-2, desmocollin-2, and plakophilin-2) [21,22], and junctophilin-2 'JPH2' [23]. All these studies were based on targeted or low-throughput experiments. A high-throughput approach is needed to systematically characterize the cardiac palmitoylome. Second, we identified DHHC enzymes expressed in the heart. We list the DHHC antibodies we have tested and those validated. We also discuss the challenges encountered when using the validated antibodies to quantify native DHHC enzymes expressed in normal and diseased hearts from different species.

2. Materials and methods

2.1. Human heart tissue and animal models

For experiments presented in Figs. 1-3, non-failing human heart samples were obtained from the Duke Human Heart Repository. For experiments presented in Fig. 6, non-failing and failing human heart samples were obtained from the Translational Cardiovascular Biobank and Repository at Washington University at St. Louis. Patient data are reported in *on-line Supplement*. Experiments using human heart tissue were approved by the Virginia Commonwealth University (VCU) Institutional Review Board (protocol HM11452). Animal models included rats (6 month old Sprague Dawley, 2–4 month- and 22–24 month-old spontaneously hypertensive rats, male), dog (mongrel, male, ~2 years old), and mice (1 month-old C57BL16). Animal use conformed to the *Guide for the Care and Use of Laboratory Animals,* and was approved by VCU Institutional Animal Care and Use committee.

2.2. Global enrichment of S-palmitoylated proteins from hearts

We used resin assisted capture (RAC) [5] to enrich S-palmitoylated proteins from the membrane-enriched fraction of heart tissue samples. Detailed description of the RAC procedure is provided in *on-line* Supplement.

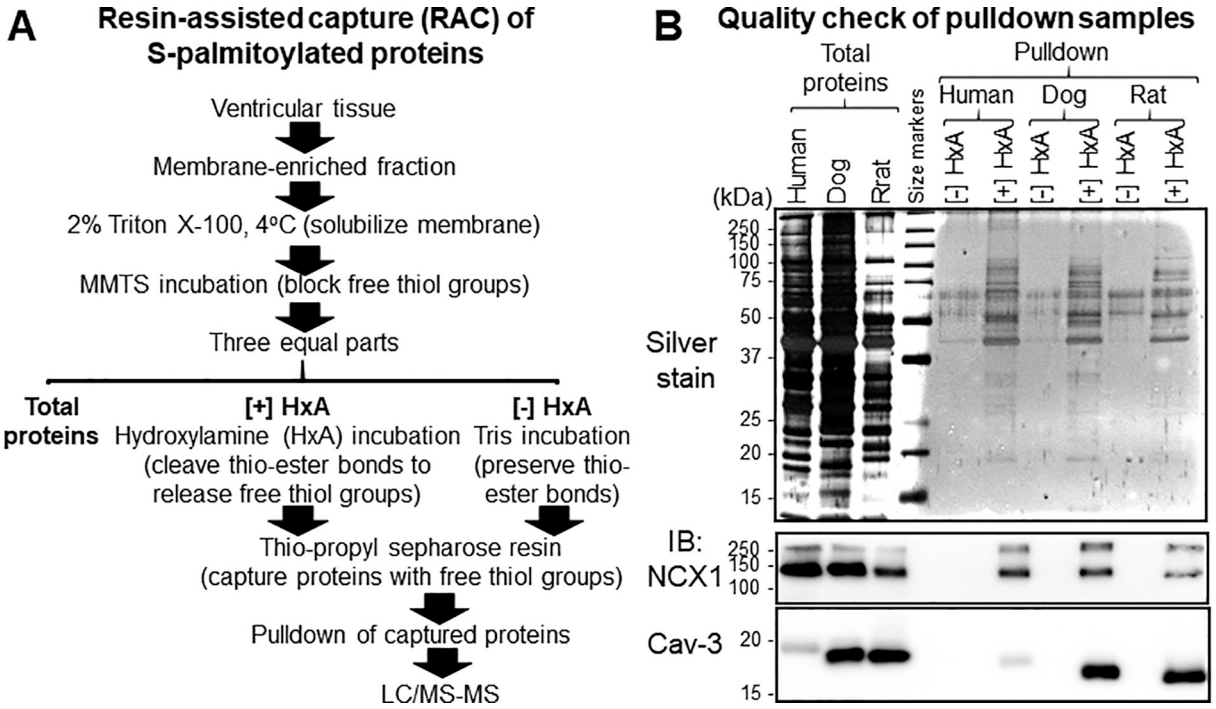

Fig. 1. Enrichment of S-palmitoylated proteins from hearts and quality check of the pulldowns. (A) Diagram of the resin-assisted capture (RAC [5]) procedure applied to membrane-enriched fraction of ventricular tissue. Tissue samples from human (three non-failing heart samples combined), dog (male mongrel, 2 years old), and rat (male Sprague Dawley, 6 months old) hearts were used. Details of the RAC procedure are in *on-line Supplement*. The [−] and [+] HxA pulldowns were used for proteomics experiments. There was no biological replicate. (B) Silver stain shows a high degree of protein enrichment in [+] HxA relative to [−] HxA pulldowns. Immunoblots (IB) show capture of known S-palmitoylated proteins (Na/Ca exchanger 'NCX1' and caveolin-3 'Cav-3') in the [+] HxA but not [−] HxA pulldowns. $n = 1$ per animal was used for the mass spec study.

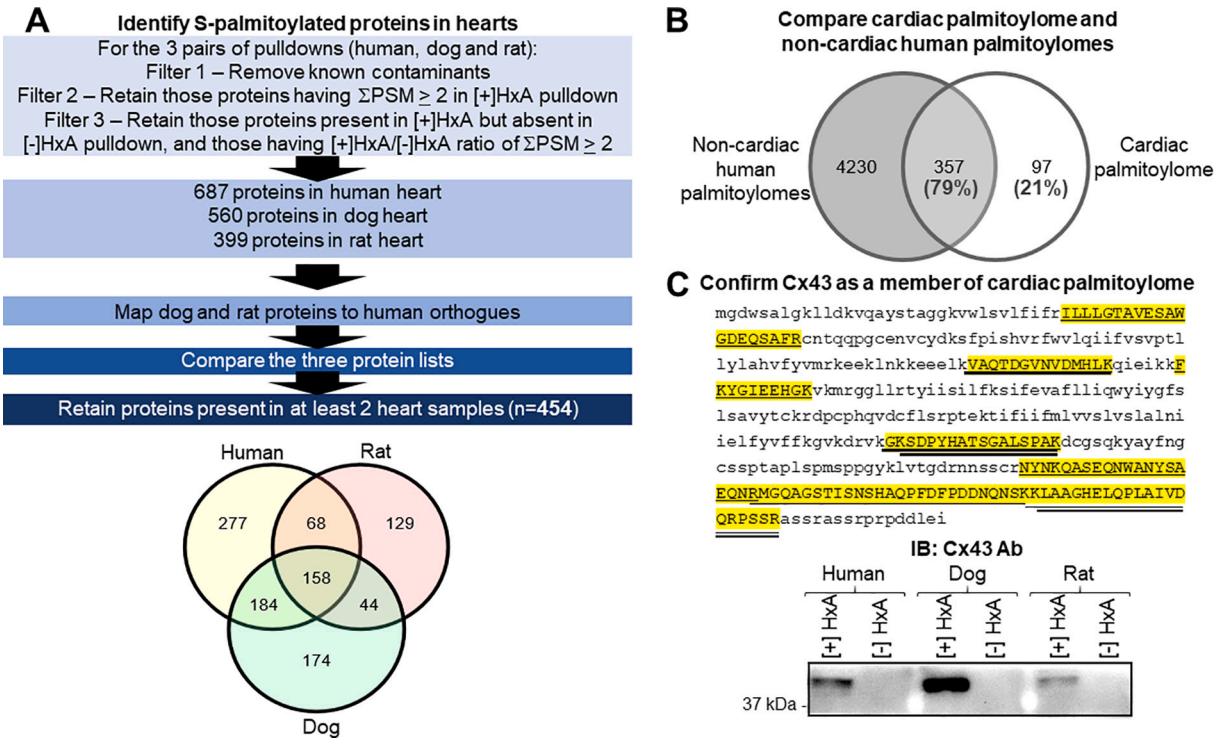

Fig. 2. Analysis of proteomics data. (A) Flowchart of data analysis. Venn diagram depicts overlaps among S-palmitoylated proteins identified in human, rat and dog hearts. There was no biological replicate. (B) Overlap between the 454 proteins in cardiac palmitoylome and 4587 proteins in non-cardiac human palmitoylomes (downloaded from SwissPalm, version 3, https://swisspalm.org) [7]. (C) Validating connexin 43 (Cx43, also known as 'gap junction α-1 protein') as a novel member of the cardiac palmitoylome. *Top*: human Cx43 amino acid sequence with peptides detected in LC/MS-MS marked by underlines. Eleven peptides were found in the human heart sample (26% coverage), and the thickness of the underlines reflects the number of detection(s): 1 to 4. *Bottom*: Immunoblot of [+] HxA and [−] HxA pulldowns probed with Cx43 mouse Ab.

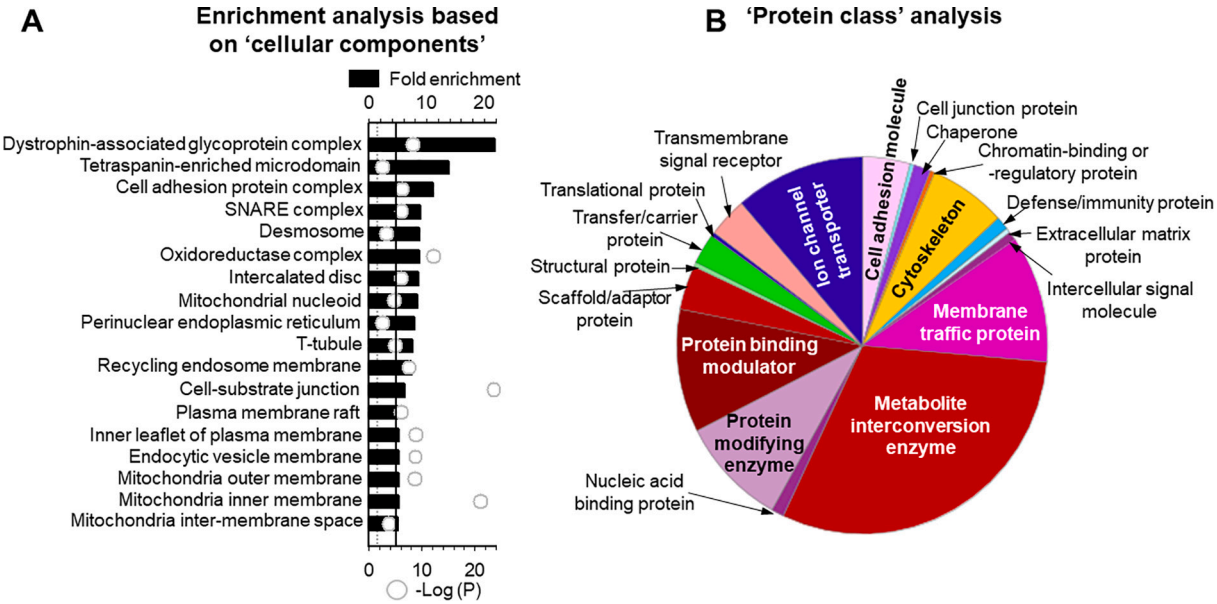

Fig. 3. Analysis of the cardiac palmitoylome. The 454 proteins were submitted to Panther System Analysis (https://pantherdb.org) [25] for statistical over-representation test and protein classification. (A) Cellular components where cardiac palmitoylome proteins are overrepresented vs a reference set of 20,851 human proteins, arranged with descending fold-enrichment (histogram, upper axis), along with their -Log(P) values (circles, lower axis). The solid black line and dotted gray line denote fold-enrichment of 5 and P vale of 0.05. (B) Pie chart of protein classification. A total of 265 proteins are matched to 18 protein classes.

2.3. Liquid chromatography and tandem mass spectrometry (LC/MS-MS)

Detailed description of LC/MS-MS is provided in *on-line* Supplement. Briefly, proteins in [−] and [+] hydroxylamine (HxA) pulldowns from the RAC procedure (Fig. 1A) were reduced, alkylated, and loaded onto an S-Trap micro column to remove LC/MS incompatible reagents. The proteins were digested with trypsin and the resulting peptides were extracted as previously described [24]. The peptides were analyzed with

an EASY nLC 1200 HPLC coupled to a Thermo Fisher Scientific Q Exactive HF-X Mass Spectrometer operated in data-dependent mode. Human and rat data were searched against the UniProt database. Dog data were searched against the RefSeq database. All searches were done using Proteome Discoverer 1.4.

2.4. COS-7 cell culture and transfection

These procedures have been described in our previous publications [13,23], and are described in details in the *on-line* Supplement.

2.5. Sodium dodecylsulfate-polyacrylamide gel electrophoresis (SDS-PAGE), silver stain, immunoblot and densitometry

The procedures of SDS-PAGE, immunoblot and densitometry have been described in our previous publications [13,23], and are described in details in *on-line* Supplement. Silver stain was carried out using Pierce Silver Stain kit, following the manufacturer's instructions.

2.6. Statistical analysis

Comparisons between normal and diseased hearts were done using 2-tailed *t*-test assuming unequal variance (Microsoft Excel).

3. Results and discussion

3.1. Global enrichment of S-palmitoylated proteins from hearts

We used the resin-assisted capture 'RAC' [5] to enrich S-palmitoylated proteins from human, dog, and rat hearts without biological replicates. The RAC procedure is diagrammed in Fig. 1A. We made three samples from each heart specimen: total proteins, [+] hydroxylamine (HxA) and [−] HxA pulldowns. HxA treatment cleaved thio-ester bonds and released free thiol groups from S-palmitoylated sites, allowing their capture by the thio-reactive resin. Although thio-ester bonds are also present in proteins cross-linked between cysteine and asparagine or glutamine side chains, the latter type of post-translational modification is much rarer than S-palmitoylation. Without HxA treatment, proteins in the [−] HxA pulldown represented non-specific binding. The [−] HxA pulldown served as negative control in proteomics and immunoblot experiments. Fig. 1B, silver stain, shows that there were much more proteins detected in the [+] HxA lane than the [−] HxA lane, indicating the effectiveness of HxA treatment in releasing free thiol groups for resin capture. Immunoblot shows that known S-palmitoylated proteins in cardiac myocytes (Na/Ca exchanger 'NCX1' [16] and caveolin-3 'Cav-3' [20]) were detected [+] HxA lane but not [−] HxA lane, supporting the specificity of resin capture. These data confirmed the high quality of [+] HxA and [−] HxA pulldowns, which were used for protein identification by LC/MS-MS.

Details of the LC/MS-MS experiments are provided in *on-line Supplement*. The raw mass spectrometry data and databases used to search proteins are accessible under MassIVE ID: MSV000085994. Excel files listing identified proteins along with detected peptide sequences are available in *on-line Supplement*.

3.2. Investigating the prevalence of S-palmitoylated proteins in hearts

Fig. 2A lists the filters used to select candidate S-palmitoylated proteins from the data set. The human, dog and rat protein identification results are available in *on-line* Tables S1, S2 and S3. Each protein list represents a snapshot of S-palmitoylated proteins present in the heart at the time of experiment. To identify a representative palmitoylated protein pool in the hearts, we matched the rat and dog proteins to human orthologs (human accessions listed in Table S2 and S3). This allowed us to compare the three protein lists and retain those present in at least two of them (Venn diagram in Fig. 2A). We defined the resulting 454 proteins operationally as a composite cardiac palmitoylome. They are listed in on-line Table S4.

Comparison of these 454 proteins with 2587 proteins previously found in 17 human palmitoylomes from non-cardiac cell types (https://swisspalm.org/) [7] shows that 79% of the composite cardiac palmitoylome overlaps with the non-cardiac human palmitoylomes (Fig. 2B). If the comparison is extended to mouse palmitoylomes (17, all from non-cardiac cell types), the degree of overlap increases to 90%.

For the validation purpose, we selected one novel candidate palmitoylated protein discovered in our analysis, connexin 43 (Cx43, also called 'gap junction α-1 protein'). Cx43 has not been found in any previous non-cardiac palmitoylomes. Inspection of peptide matches shows a 26% coverage in human cardiac palmitoylome (Fig. 2C, top). The coverages are 33% and 36% in rat and dog cardiac palmitoylomes (Tables S2 and S3). Immunoblot of the 3 pairs of [−] HxA and [+] HxA pulldown shows that Cx43 is present in all [+] HxA but absent in [−] HxA (Fig. 2C, bottom). In conclusion, our composite cardiac palmitoylome is validated by the high degree of overlap with previously identified human and mouse palmitoylomes, and the confirmation of a novel palmitoylated protein, Cx43.

3.3. Functional implication of the composite cardiac palmitoylome

We submitted the list of 454 proteins to Panther Classification System (http://www.pantherdb.org/) [25] for statistical analysis and protein classification. Because S-palmitoylation is a major driving force for protein trafficking and distribution in cells, we analyzed the cardiac palmitoylome by statistical overrepresentation test based on Gene Ontology (GO) terms 'cellular component' (Fig. 3A). The 454 proteins were compared against 20,851 human proteins, and the fold-enrichment in cardiac palmitoylome in terms of the number of proteins localized in different cellular components was calculated along with *p*-values (based on Fisher's exact test) [25]. The Panther analysis reports cellular components in different groups based on relatedness, and within each group, there is a hierarchy from the most specific cellular component in the group to less specific components with decreasing fold-enrichment (Fig. S1A). We excluded those cellular component groups deemed irrelevant for cardiac myocytes, and those cellular components relevant for cardiac myocytes but with fold-enrichment <5. This information is listed in Fig. S1B. For each of the remaining cellular component groups, we chose the broadest level in the hierarchy where fold-enrichment was >5. These data are presented in Fig. 3A. The protein list is in *on-line* Table S5.

This cellular component analysis shows that the functional roles of cardiac palmitoylome can be divided into three categories. The first category is 'universal roles' shared between cardiac and non-cardiac palmitoylomes. These include organization of membrane microdomains (plasma membrane raft, tetraspanin-enriched microdomain, inner leaflet of the plasma membrane where signaling molecules, e.g. heterotrimeric G proteins, bind), cell-substrate and cell-cell adhesion junctions, vesicular trafficking, and organization of mitochondrial protein complexes in the outer and inner membranes and in the intermembrane space. The second category is 'striated muscle-related roles'. These are proteins involved in the organization and function of t-tubules and costameres (the dystrophin-glycoprotein complex and the integrin-vinculin-talin complex [26]). These two cellular components are specific for striated muscles, i.e. skeletal and cardiac muscles. The third category is 'cardiac-specific role', and includes proteins involved in the organization and function of intercalated disc ('ICD', including components of desmosomal and adherens junctions [21,22], Cx43, and Nav1.5 [11]). ICD is a subcellular domain specific for the myocardial syncytium, where adjacent myocytes are mechanically linked through desmosomal and adherens junctions and action potentials are propagated between myocytes through the gap junctional channels.

The cellular component analysis tells us *where* the palmitoylated proteins are in myocytes. A complementary analysis, 'protein class', tells

us *what* they are. Out of the 454 proteins, 265 were mapped to 18 protein classes (Fig. 3B, and protein list in Table S5). In terms of the protein abundance among the classes, the top five are: metabolic interconversion enzymes (31%), channels/transporters (11%), membrane traffic proteins (11%), protein-binding activity modulators (11%), and protein modifying enzymes (9%).

3.4. Identifying DHHC enzymes expressed in the heart

How is the degree of protein palmitoylation regulated in the heart? To answer this question, we need to know which of the 23 palmitoylating (DHHC) enzymes are expressed in cardiac myocytes. A previous study has quantified mRNAs of DHHC genes in the rat heart [19]. However, proteins are direct operators of enzymatic function, and mRNA levels may not be linearly related to the protein levels. Table S6 lists the twenty four DHHC antibodies we have tested. We focused on the so-called 'Prestige Abs' developed by the Human Protein Atlas project (https://www.proteinatlas.org). DHHC19 Ab was from a difference source because no Prestige Ab was available. There was no commercial Ab targeting DHHC23 at the time of our experiments.

All the DHHC Abs were raised against antigens 'Ag' derived from human DHHC proteins. Our analysis showed that except three, all the other antigens are 90–100% conserved in orthologs across the 3 animal species included in this study: mouse, rat and dog. Antigens for DHHC3, DHHC16, and DHHC19 are 72–86% conserved in orthologs of the 3 species (Table S6).

We first tested whether the DHHC Abs can detect their targets encoded by mouse cDNAs expressed in COS-7 cells. These mouse DHHC enzymes are tagged with hemagglutinin 'HA' epitope, allowing us to use HA mAb immunoblot as positive control. Untrasnfected COS-7 cells served as negative control. Fig. 4 summarizes our findings. A DHHC Ab was deemed '*validated*' if it detected the same band(s) as in HA mAb immunoblot (e.g. DHHC2 Ab). Because COS-7 cells are expected to express native DHHC enzymes that could be detected by DHHC Abs in untransfected cells, those Abs that detected bands in both transfected and untransfected cells with higher intensity in the former (e.g. DHHC5 Ab) were also deemed '*validated*'. A total of thirteen DHHC Abs were validated for their ability in detecting targets expressed in COS-7 cells (highlighted by yellow shading in Fig. 4, and so marked in Table S6).

Fig. 4 shows that in the cases of DHHC2, DHHC9, DHHC18, DHHC20, and DHHC22, a single DHHC cDNA produced multiple bands in immunoblots. There are precedents in the literature [19,27]. This prompted us to search the protein database of National Center for Biotechnology Information (NCBI). Each of the DHHC enzymes has multiple isoforms. Our search results on human DHHC isoforms are summarized in Table S7, and amino acid sequence alignments are reported in *on-line Supplement*. These results indicate that the mouse cDNAs expressed in COS-7 cells can be alternatively spliced, producing multiple proteoforms.

We then used the thirteen validated DHHC Abs to probe whole tissue lysates prepared from human, dog and rat hearts. We used 'Ag pre-adsorption' to help us distinguish authentic DHHC bands (band intensity diminished by Ag pre-adsorption) from non-specific bands in immunoblots. BLAST of the Ag sequences against the NCBI protein database confirmed that they are all specific for their target DHHC proteins. Fig. 5 depicts three examples of authenticating immunoblot bands detected by DHHC Abs. Fig. S2 summarizes the Ag pre-adsorption tests of all thirteen DHHC Abs. In total, we detected eleven DHHC enzymes expressed in the heart: DHHC1, DHHC2, DHHC4, DHHC5, DHHC7, DHHC8, DHHC9, DHHC17, DHHC18, DHHC20, and DHHC21.

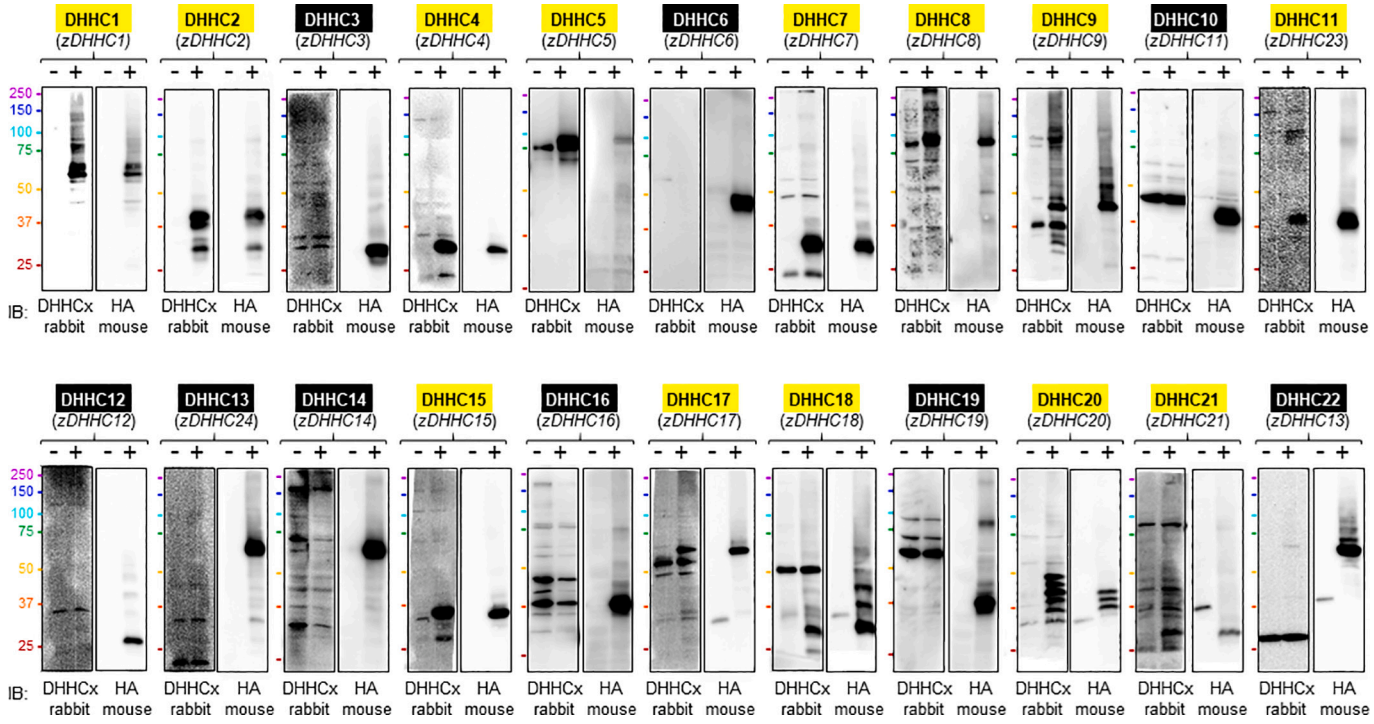

Fig. 4. Testing the ability of DHHC antibodies in detecting their targets in immunoblots. Mouse cDNAs encoding DHHC1 - DHHC22 (also known as *zDHHC* with not identical numbering, noted in parentheses), with a hemagglutinin (HA) epitope tag, were transfected into COS-7 cells. Untransfected COS-7 cells served as negative control. Whole cell lysates were fractionated by SDS-PAGE and the PVDF membranes were probed with DHHC rabbit antibodies. The PVDF membranes were stripped and reprobed with HA mouse antibody. Shown are immunoblot images of DHHC rabbit and HA mouse antibodies side-by-side, with '-' and '+' above noting untransfected and transfected cell samples. Size marker bands are shown next to the left most panels, with sticks of the same colors shown left to the other panels. Yellow and black shadings denote 'validated' and 'not validated' DHHC antibodies, respectively, for immunoblot detection. (For interpretation of the references to colour in this figure legend, the reader is referred to the web version of this article.)

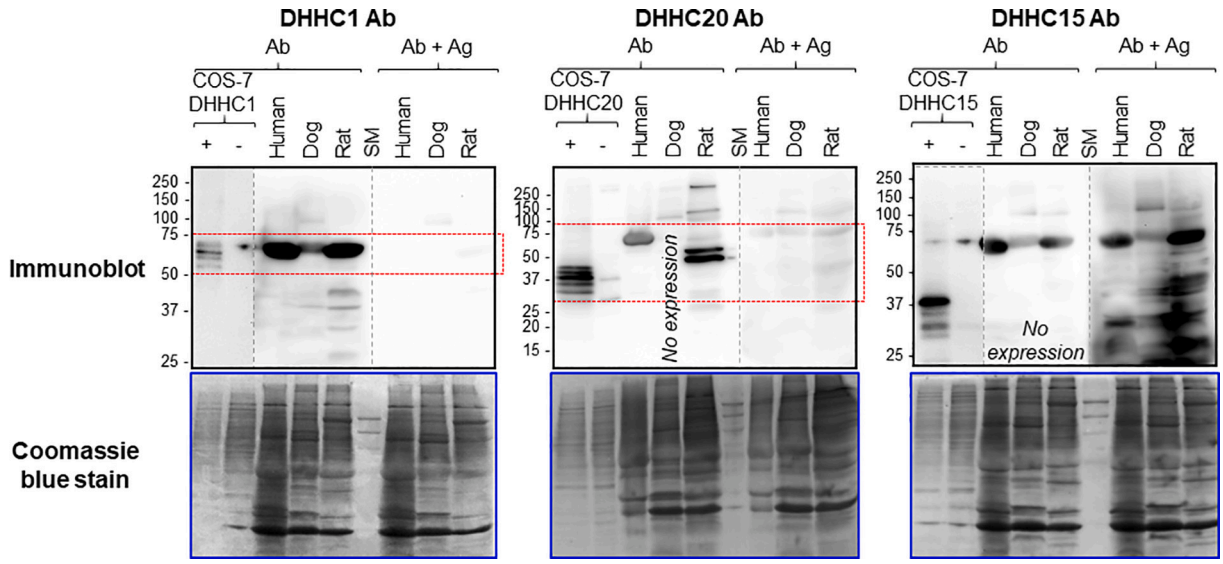

Fig. 5. Using antibody pre-adsorption by antigen (Ag) to authenticate immunoblot bands from cardiac whole tissue lysates detected by DHHC antibodies. Equal amounts of whole tissue lysates from human, dog and rat hearts were loaded into two sets of lanes separated by a size marker (SM) lane. Whole cell lysates from COS-7 expressing mouse DHHC protein and untransfected cells ('+' and '-' respectively) were included as references. The proteins were fractionated by SDS-PAGE and blotted to PVDF membranes. The PVDF membranes were cut along the SM lane. The left portion was probed with DHHC Ab (100× dilution). The right portion was probed with the same DHHC Ab (100× dilution) preincubated with Ag (20× dilution) for 1 h at room temperature with rotation. The procedures of primary and secondary Ab incubation and ECL detection were carried out side-by-side to ensure that no untoward variations between the 'Ab' and 'Ab+Ag' immunoblots were introduced during these procedures. Proteins remaining in the gels were stained with Coomassie blue to ensure even loading between Ab and Ab+Ag lanes (lower row). Immunoblot bands whose intensities were diminished by Ag pre-adsorption represent proteins carrying the Ag sequences and thus are authenticated as DHHC bands, highlighted by red dotted rectangles. Dotted vertical lines denote the boundaries between the Ab and Ab+Ag portions. For DHHC1 and DHHC15, images of the COS-7 '+' and '-' lanes were from a different brightness/contrast setting (noted by dashed borders) to make them better match the images of the other lanes. A summary of authenticated immunoblot bands detected by DHHC antibodies is presented in Fig. S2. (For interpretation of the references to colour in this figure legend, the reader is referred to the web version of this article.)

3.5. Challenges in using DHHC antibodies to quantify native enzymes in hearts

We further tested the usefulness of the DHHC Abs in studying DHHC enzyme remodeling in normal and diseased hearts. We used an animal model of chronic hypertension with hypertrophy (spontaneously hypertensive rat, SHR) [28]. Six young SHR (2–4 months of age) and six old SHR (22–24 months of age) were compared. Young SHR animals are relatively healthy with mild myocardial hypertrophy relative to age-matched normotensive Wistar Kyoto rats (heart-to-body weight ratio, in g/kg: 4.42 ± 0.20, $n = 14$, vs 3.56 ± 0.34, $n = 12$, $p = 0.03$). Old SHR developed severe myocardial hypertrophy (heart-to-body weight ratio 5.75 ± 0.42, $n = 16$, $p = 0.02$ vs young SHR), and often exhibited overt signs of heart failure (left atrial thrombosis, increased interstitial fibrosis [29]). We also compared human non-failing donor hearts ($n = 6$) and end-stage failing hearts (n = 6, 3 ischemic and 3 non-ischemic, patient data in *on-line Supplement*). Whole tissue lysates were prepared and fractionated by SDS-PAGE, along with positive controls of COS-7 cells.

Fig. 6A depicts immunoblot images. Authenticated bands, based on Fig. 5 and S2, are marked by red dotted boxes and were included in densitometry quantification. The band intensities were corrected for minor loading variations revealed by Coomassie blue stain of the gels (Fig. 6B), and normalized by the mean value of band intensities from controls of the same immunoblots, i.e. young SHR for the SHR hearts and non-failing for the human hearts. Densitometry quantification and statistical analysis are shown in Fig. 6C.

3.6. Challenges and suggestions on how to move forward

Fig. 6A illustrates the challenge in using validated DHHC Abs to address a new question: whether or how DHHC enzymes are remodeled in diseased hearts? DHHC enzymes may exist in multiple proteoforms due to alternative RNA splicing (Table S7) and post-translational modifications [30]. Some DHHC enzymes may dimerize or oligomerize with altered enzymatic activity [31]. These events may serve the purpose of diversifying the DHHC enzyme repertoire, so that protein products from the 23 DHHC genes in human can fulfill the function of S-palmitoylating ~4600 human proteins [7]. These events, in addition to alterations in DHHC gene transcription, protein distribution and degradation, may all be subject to remodeling in diseased hearts, and DHHC remodeling may be species- and etiology-dependent. To fully characterize DHHC proteoforms in the heart requires 'top-down' proteomics, that analyzes intact proteins instead of peptide fragments in conventional 'bottom-up' proteomics [32]. The field of top-down proteomics has made major stride in recent years in instrumentation and methodology. However, it requires protein purification and works best for proteins <30 kDa in size.

There are other limitations in our experiments that impact data interpretation. Because our starting materials were membrane-enriched fractions, our results might be biased toward membraned cellular components. The RAC enrichment procedure was based on the assumptions that all free thiol groups had been protected, and all S-palmitoylated sites had been cleaved by HxA. Neither assumption can be independently verified.

Our proteomic experiments did not identify S-palmitoylation sites in the cardiac palmitoylome, while studies have suggested that palmitoylation of different Cys side chains can exert differential functional impacts [23]. To resolve this issue requires a targeted approach: when proteins of interest are identified where changes in their S-palmitoylation are linked to physiological or pathological consequences, one can predict putative S-palmitoylation sites (e.g. CSS-Palm, GPS-Palm), mutate the Cys side chain(s) at single or combined sites, quantify resulting changes in the degree of S-palmitoylation, and investigate the functional impacts. The alternative approach is top-down proteomics discussed above [32], that requires protein purification as the first step and thus is suitable after proteins of interest have been identified.

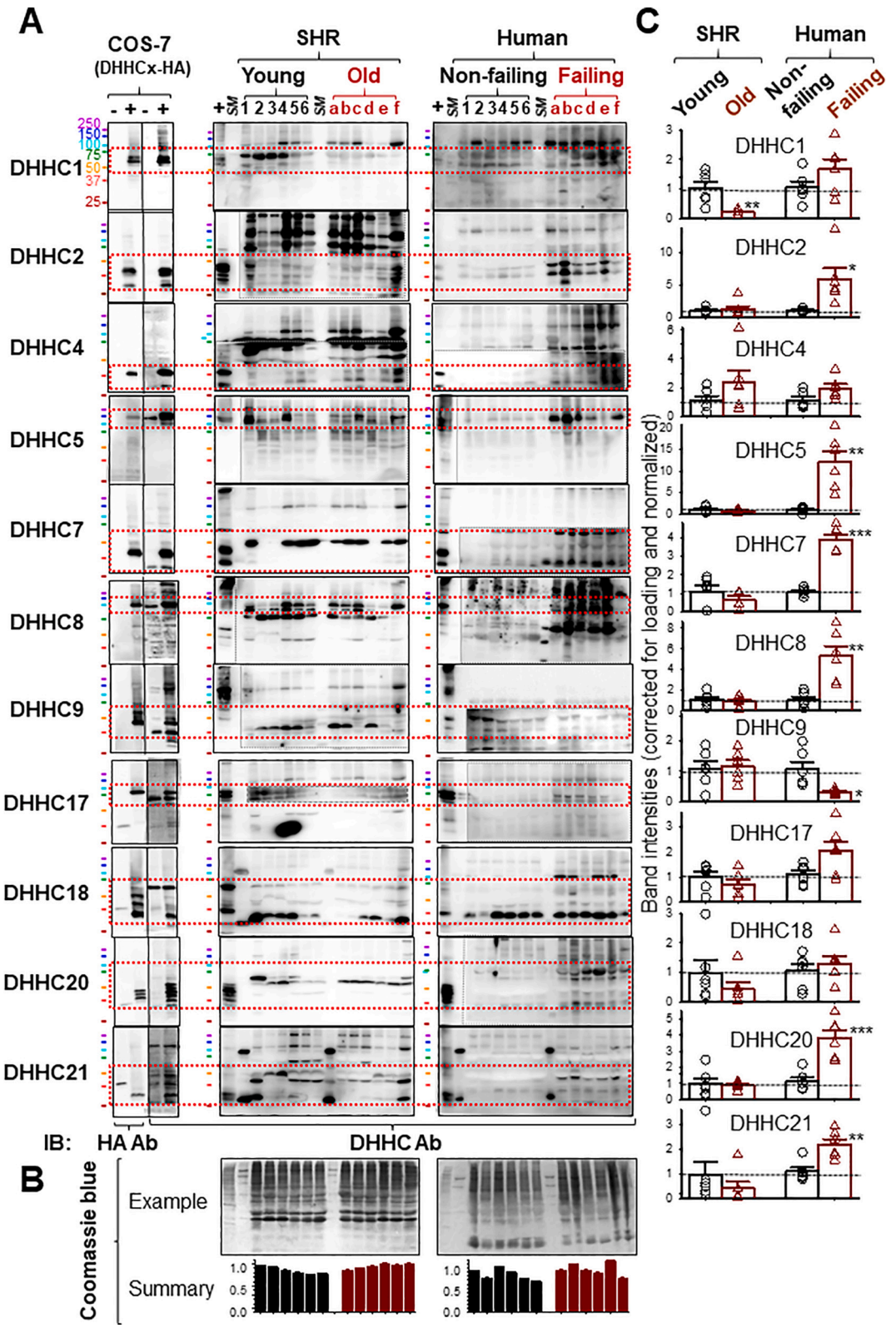

(caption on next page)

Fig. 6. Using DHHC antibodies to study remodeling of DHHC enzymes in chronically stressed hearts. (A) Immunoblot images. Whole tissue lysates were prepared from six young (2–4 months) and six old (22–24 months) male SHR hearts, and from six non-failing and six failing human hearts (3 ischemic and 3 non-ischemic heart failure, patient data in *on-line Supplement*). Each immunoblot included whole cell lysate from COS-7 cells expressing the target DHHC enzyme as a reference (left most lane in each immunoblot, marked '+'). Heart tissue lysate samples, along with size marker (SM) lanes, are noted on top. DHHC Ab validation data from Fig. 4 are also shown to the left, with HA Ab or DHHC Ab marked below the immunoblots. The targets of DHHC antibodies are noted on the left. The size marker bands are colour coded and labeled on the left of the DHHC1 immunoblot. Authenticated immunoblot bands (based on Fig. 5 and Fig. S2) are marked by red dotted boxes. Dashed vertical lines denote boundaries between COS-7 and heart tissue lysate lanes from the same immunoblots, where the brightness/contrast was separately adjusted to match their background and band intensities for illustration purpose. (B) Example of Coomassie blue stain and summary of densitometry quantification of eleven polyacrylamide gels from experiments shown in (A). The Coomassie blue intensities of individual lanes in each of the gels were normalized by the mean value of the same gel. (C) Densitometry quantification of authenticated immunoblot bands shown in (A). The band intensities were background-subtracted, corrected for minor loading variations (based on B) and normalized by the mean value of controls: young SHR for SHR data, and non-failing for human heart data. Dashed horizontal lines denote value of '1'. Symbols represent data from individual hearts; histogram bars represent mean ± SE. *t*-test between young vs old SHR hearts, or between non-failing vs failing human hearts: * $p < 0.05$, ** $p < 0.01$, *** $p < 0.001$. (For interpretation of the references to colour in this figure legend, the reader is referred to the web version of this article.)

Finally, an integral part of studying DHHC enzymes in cardiac myocytes is to identify their 'territories': DHHC enzymes are integral membrane proteins; their substrates need to traffic to where the enzymes are for palmitoylation [33–35]. Although the distribution patterns of DHHC enzymes have been reported for fibroblast-like cells, cardiac myocytes with their tightly organized sarcomeres and well-defined sarcolemma components require their own investigation. We have validated twelve DHHC Abs for immunofluorescence (IF) detection of their targets (Table S6). To authenticate these IF signals requires Ab-free detection of DHHC enzymes expressed in myocytes. This is achievable by using viral vectors to express fluorescent protein (FP) tagged DHHC enzymes in myocytes and use fluorescence microscopy to monitor their distribution pattern.

3.7. Summary

We provide the following resources for investigators interested in studying protein S-palmitoylation and its regulation in the heart: palmitoylome data repository and analysis, proteins found in a composite cardiac palmitoylome and their classification (Tables S1-S5), twenty four commercial DHHC antibodies tested and those validated for immunoblot and immunofluorescence detection, along with homology of antigen sequences in human, mouse, rat and dog orthologs (Table S6), and information about splice variants in DHHC enzymes (Table S7). We also discuss challenges encountered in these experiments, and suggest tools that should be developed to overcome the challenges.

Supplementary data to this article can be found online at https://doi.org/10.1016/j.yjmcc.2021.02.007.

Funding sources

This study was supported by NIH/NHLBI (HL128610 and HL96962).

Acknowledgements

Confocal microscopy was performed at the Virginia Commonwealth University – Department of Neurobiology & Anatomy Microscopy Facility, supported in part by National Institute of Neurological Disorders and Stroke at National Institutes of Health (NIH-NINDS) Center Core Grant 5P30NS047463. The mass spectrometric experiments were in part supported by Grossman School of Medicine, New York University. The authors thank Jeanne Nerbonne, Kory Lavine and colleagues at Washington University for providing human ventricular tissue samples through the Translational Cardiovascular Biobank and Repository, supported in part by Clinical and Translational Science Award from National Institutes of Health (NIH CTSA) Grant #UL1 TR002345 and the Children's Discovery Institute.

References

[1] Y. Fukata, T. Murakami, N. Yokoi, M. Fukata, Local palmitoylation cycles and specialized membrane domain organization, Curr. Top. Membr. 77 (2015) 97–141.
[2] L.H. Chamberlain, M.J. Shipston, The physiology of protein S-acylation, Physiol. Rev. 95 (2015) 341–376.
[3] C. Aicart-Ramos, R.A. Valero, I. Rodriguez-Crespo, Protein palmitoylation and subcellular trafficking, Biochim. Biophys. Acta 1808 (2011) 2981–2994.
[4] J. Wan, A.F. Roth, A.O. Bailey, N.G. Davis, Palmitoylated proteins: purification and identification, Nat. Protoc. 2 (2007) 1573–1584.
[5] M.T. Forrester, D.T. Hess, J.W. Thompson, R. Hultman, M.A. Moseley, J.S. Stamler, R.J. Casey, Site-specific analysis of protein *S* -acylation by resin-assisted capture, J. Lipid Res. 52 (2011) 393–398.
[6] H.C. Kolb, M.G. Finn, K.B. Sharpless, Click chemistry: diverse chemical function from a few good reactions, Agnew. Chem. Int. Ed. Engl. 40 (2001) 2004–2021.
[7] M. Blanc, F.P.A. David, F.G. van der Goot, SwissPalm 2: protein S-palmitoylation database, in: Methods and Protocols, Methods in Molecular Biology, 2019, pp. 203–214.
[8] L.D. Hamel, B.J. Lenhart, D.A. Mitchell, R.G. Santos, M.A. Guilianotti, R. J. Deschenes, Identification of protein palmitoylation inhibitors from a scaffold ranking library, Comb. Chem. High Throughput Sceen. 19 (2016) 262–274.
[9] M.J. Lin, M. Fine, J.-Y. Lu, S.L. Hofmann, G. Frazier, D.W. Hilgemann, Massive palmitoylation-dependent endocytosis during reoxygenation of anoxic cardiac muscle, eLife 2 (2013), https://doi.org/10.7554/eLife.01295.
[10] R. Joehanes, S. Ying, T. Huan, A.D. Johnson, N. Raghavachari, R. Wang, P. Liu, K. A. Woodhouse, S.K. Sen, K. Tanriverdi, P. Courchesne, J.E. Freedman, C. J. O'Donnell, D. Levy, P.J. Munson, Gene expression signatures of coronary heart disease, Arterioscler. Thromb. Vasc. Biol. 33 (2013) 1418–1426.
[11] Z. Pei, Y. Xiao, J. Meng, A. Hudmon, T.R. Cummins, Cardiac sodium channel palmitoylation regulates channel availability and myocyte excitability with implications for arrhythmia generation, Nat. Commun. (2016), https://doi.org/10.1038/ncomms12035.
[12] H.K. Jindal, E.J. Folco, G.X. Liu, G. Koren, Posttranslational modification of voltage-dependent potassium channel Kv1.5: COOH-terminal palmitoylation modulates its biological properties, Am. J. Phys. 294 (2008) H2012–H2021.
[13] A. Murthy, S.W. Workman, M. Jiang, J. Hu, I. Sifa, T. Bernas, W. Tang, I. Deschenes, G.-N. Tseng, Dynamic palmitoylation regulates trafficking of K channel interacting protein 2 (KChIP2) across multiple subcellular compartments in cardiac myocytes, J. Mol. Cell. Cardiol. 135 (2019) 1–9.
[14] H.-Q. Yang, W. Martinez-Rotiz, J. Hwang, X. Fan, T.J. Cardozo, W.A. Coetzee, Palmitoylation of the KATP channel Kir6.2 subunit promotes channel opening by regulating PIP2 sensitivity, PNAS 117 (2020) 10593–10602.
[15] N. Qin, D. Platano, R. Olcese, J.L. Costantin, E. Stefani, L. Birnbaumer, Unique regulatory properties of the type 2a Ca^{2+} channel β subunit caused by palmitoylation, PNAS 95 (1998) 4690–4695.
[16] L. Reilly, J. Howie, K. Wypijewski, M.L.J. Ashford, D.W. Hilgemann, W. Fuller, Palmitoylation of the Na/Ca exchanger cytoplasmic loop controls its inactivation and internalization during stress signaling, FASEB J. 29 (2015) 4532–4543.
[17] T. Zhou, J. Li, P. Zhao, H. Liu, D. Jia, H. Jia, L. He, Y. Cang, S. Boast, Y.-H. Chen, H. Thibault, M. Scherrer-Crosbie, S.P. Goff, B. Li, Palmitoyl acyltransferase Aph2 in cardiac function and the development of cardiomyopathy, PNAS 112 (2015) 15666–15671.
[18] J. Liu, G. Carcia-Cardena, W.C. Sessa, Palmitoylation of endothelial nitric oxide synthase is necessary for optimal stimulated release of nitric oxide: implications for caveolae localization, Biochemistry 35 (1996) 13277–13281.
[19] J. Howie, L. Reilly, N.J. Fraser, J.M.V. Walker, K.J. Wypijewski, M.L.J. Ashford, S. C. Calaghan, H. McClafferty, L. Tian, M.J. Shipston, A. Boguslavskyi, M.J. Shattock, W. Fuller, Substrate recognition by the cell surface palmitoyl transferase DHHC5, PNAS 111 (2014) 17534–17539.
[20] D.J. Dietzen, W.R. Hastings, D.M. Lublin, Caveolin is palmitoylated on multiple cysteine residues, J. Biol. Chem. 270 (1995) 6838–6842.
[21] B.J. Roberts, R.A. Svoboda, A.M. Overmiller, J.D. Lewis, A.P. Kowalczyk, M. G. Mahoney, K.R. Johnson, J.K.I. Wahl, Palmitoylation of desmoglein 2 is a regulator of assembly dynamics and protein turnover, J. Biol. Chem. 291 (2016) 24857–24865.
[22] B.J. Roberts, K.E. Johnson, K.P. McGuinn, J. Saowapa, R.A. Svoboda, M. G. Mahoney, K.R. Johnson, J.K.I. Wahl, Palmitoylation of plakophilin is required for desmosome assembly, J. Cell Sci. 127 (2014) 3782–3793.
[23] M. Jiang, J. Hu, F.K.H. White, J. Williamson, A.S. Klymchenko, A. Murthy, S. W. Workman, G.-N. Tseng, S-palmitoylation of junctophilin-2 is critical for its role

in tethering the sarcoplasmic reticulum to the plasma membrane, J. Biol. Chem. 294 (2019) 13487–13501.
[24] M.D. Keller, K.L. Ching, F.-X. Liang, A. Dhabaria, K. Tam, B.M. Ueberheide, D. Unutmaz, V.J. Torres, K. Cadwell, Decoy exosomes provide protection against bacterial toxins, Nature 579 (2020) 260–264.
[25] H. Mi, A. Muruganujan, D. Ebert, X. Huang, P.D. Thomas, PANTHER version 14: more genomes, a new PANTHER GO-slim and improvements in enrichment analysis tools, Nucleic Acids Res. 47 (2019) D419–D426.
[26] C.A. Henderson, C.G. Gomez, S.M. Novak, L. Mi-Mi, C.C. Gregorio, Overview of the muscle cytoskeleton, Comprehen. Physiol. 7 (2017) 891–944.
[27] Y. Ohno, A. Kihara, T. Sano, Y. Igarashi, Intracellular localization and tissue-specific distribution of human and yeast DHHC cysteine-rich domain-containing, Biochim. Biophys. Acta 1761 (2006) 474–483.
[28] S.A. Doggrell, L. Brown, Rat models of hypertension, cardiac hypertrophy and failure, Cardiovasc. Res. 39 (1998) 89–105.
[29] M. Jiang, Y.-H. Wang, G.-N. Tseng, Adult ventricular myocytes segregate KCNQ1 and KCNE1 to keep the I_{Ks} amplitude in check until when larger I_{Ks} is needed, Circ. Arrhythm. Electrophysiol. 10 (2017), e005084.
[30] F. Zmuda, L.H. Chamberlain, Regulatory effects of post-translational modifications on zDHHC S-acyltransferases, J. Biol. Chem. (2020), https://doi.org/10.1074/jbc.REV120.014717. In Press.
[31] J. Lai, M.E. Linder, Oligomerization of DHHC protein S-acyltransferases, J. Biol. Chem. 288 (2013) 22862–22870.
[32] T.K. Toby, L. Fornelli, N.L. Kelleher, Progress in top-down proteomics and the analysis of proteoforms, Annu. Rev. Anal. Chem. 9 (2016) 499–519.
[33] O. Rocks, A. Peyker, M. Kahms, P.J. Verveer, C. Koerner, M. Lumbierres, J. Kuhlmann, H. Waldmann, A. Wittinghofer, P.I.H. Bastiaens, An acylation cycle regulates localization and activity of palmitoylated Ras isoforms, Science 307 (2005) 1746–1752.
[34] G.S. Brigidi, B. Santyr, J. Shimell, B. Jovellar, S.X. Bamji, Activity-regulated trafficking of the palmitoyl-acyl transferase DHHC5, Nat. Commun. 6 (2015) 8200.
[35] J. Naritake, Y. Fukata, T. Iwanaga, N. Hosomi, R. Tsutsumi, N. Matsuda, H. Tani, H. Iwanari, Y. Mochizuki, T. Kodama, Y. Matsuura, D.S. Bredt, T. Hamakubo, M. Fukata, Mobile DHHC palmitoylating enzyme mediates activity-sensitive synaptic targeting of PSD-95, J. Cell Biol. 186 (2009) 147–160.